Title

A new phantom and empirical formula for apparent diffusion coefficient measurement of a 3 tesla MRI scanner

MARINA HARA[1], MASAHIRO KURODA[2], YUICHI OHMURA[2], HIDENOBU MATSUZAKI[3], TOMOKI KOBAYASHI[2], JUN MURAKAMI[3], KAZUNORI KATASHIMA[1], MASAKAZU ASHIDA[1], SEIICHIRO OHNO[4], and JUN-ICHI ASAUMI[1, 3]

[1]Department of Oral and Maxillofacial Radiology, Graduate School of Medicine, Dentistry and Pharmaceutical Sciences, [2] Radiological Technology, Graduate School of Health Sciences, [3]Department of Oral Diagnosis and Dentomaxillofacial Radiology, [4]Central Division of Radiology, Okayama University Hospital, Okayama University, 2-5-1 Shikata-cho, Okayama 700-8558, Japan

Correspondence to: Dr Masahiro Kuroda, Faculty of Health Sciences, Graduate School of Health Sciences, Okayama University, 2-5-1 Shikata-cho, Okayama 700-8558, Japan
E-mail: kurodamd@cc.okayama-u.ac.jp

Abstract

The aim of this study was to create a new phantom for a 3 tesla (T) magnetic resonance (MR) device for apparent diffusion coefficient (ADC) calculation using diffusion-weighted imaging (DWI), and to mimic ADC values of normal and tumor tissues at various temperatures including physiological body temperature of 37 °C. We made the phantom using sucrose of several concentrations from 0 to 1.2 M and performed DWI under monitoring the various phantom temperature. We calculated the accurate ADC values using DWIs of phantoms, and made an empirical formula to calculate the ADC values of phantoms from arbitrary sucrose concentration and arbitrary phantom temperature. The empirical formula could produce the ADC values of the range from 0.33–3.02 × 10^{-3} mm^2/sec, which covered the range of ADC values of human body that were measured clinically by 3T MR imaging in the previous studies. Our phantom and empirical formula might be available to mimic the ADC values of the clinical human lesion by 3T MR imaging.

Key words: sucrose, phantom, apparent diffusion coefficient value, diffusion-weighted imaging, magnetic resonance imaging, 3 tesla

Introduction

Magnetic resonance (MR) diffusion-weighted imaging (DWI) has been increasingly performed for clinical purposes such as the detection of tumors and cerebrovascular diseases. The apparent diffusion coefficient (ADC) value, which is calculated based on DWI using several b-values, is useful for discriminating whether the lesion is benign or malignant and determining a therapeutic effect of a tumor. Recently popularized 3 tesla (T) MR devices show a performance advantage when calculating accurate ADC values. Several clinical studies have revealed that ADC values from 3T MR imaging have the diagnostic value as a quantitative parameter (1-8). However, to our knowledge there is no report of an ADC phantom for 3T MR imaging. Regarding ADC phantoms for 1.5T MR imaging, Tamura, *et al.* (9) reported on a phantom that used gelatin and sucrose. Matsuya, *et al.* (10) reported on a phantom using polyethylene glycol for 1.5T MR imaging, and created empirical formulas to calculate polyethylene glycol concentration, which provide arbitrary ADC values at any measurement temperature. In principle, the ADC value of a phantom differs due to its temperature. In the present study, we developed an ADC phantom using sucrose for 3T MR imaging, which produces arbitrary ADC values due to a range of phantom temperature (28–39 °C), which includes physiological body temperature. This is the first temperature-controlled ADC phantom for 3T MR imaging. It mimics ADC values of normal and tumor tissues of the human body, and the developed empirical formula enables the calculation of sucrose concentration that provides arbitrary ADC values at any phantom temperature.

Materials and methods

Sucrose phantoms

To create sucrose phantoms, sucrose (S0389-500G, Sigma, St. Louis, MO), NaN_3 (28-1789-5, Sigma-Aldrich Co., Tokyo, Japan) as an antiseptic, and distilled water were heated and stirred until dissolved. The solution was cooled, and the final concentrations of sucrose and NaN_3 were adjusted to be 0.2, 0.4, 0.6, 0.8, 1.0 and 1.2 M, and 0.03 w/w%. These solutions were filled into phantom cases (No1-4628-11, AS ONE Co., Osaka, Japan; Fig. 1(A)) as sucrose phantoms.

Preparation for MR imaging of sucrose phantoms

Sucrose phantoms were placed into a container filled with 0.9 M sucrose solution and 0.03 w/w% NaN_3. The container could hold a maximum of 16 phantoms (Fig. 1(B)).

Heating system

The phantom case container was enclosed in a heating box (Fig. 1(C)) made of Styrofoam that was created in-house. The container was heated in the gantry of an MR scanner via a tube that was connected to a circulating temperature-regulated water bath (Thermo-Mate BF-41; Yamato Scientific Co., Ltd., Tokyo, Japan; Fig. 1(D)) to keep the desired phantom temperature constant during MR imaging.

Real-time phantom temperature monitoring

Optical fiber thermometers (Fluoroptic™ thermometer m600; Luxtron Co., Mountain View, CA; Fig. 1(E)) were put into phantoms. Phantom temperature was monitored every 30 s during MR imaging to ensure a constant temperature.

MR imaging

A clinical 3T MRI unit (Magnetom Skyra; Siemens, Erlangen, Germany) with a head coil was used for MR imaging. DWIs were acquired by a three-scan trace, in the phase-encoding, readout and slice-selective directions, via a single-shot echo-planar imaging sequence. The scan parameters were set as follows: 8000 ms of relation time, 100 ms of echo time, 220 × 220 mm field of view, 160 × 112 matrix, b values of 0, 300, 600, 900, 1200, 1500, 1800, 2100, 2400, 2700, and 3000 s/mm^2, a thickness of 5 mm, one excitation number, 26.2 ms diffusion gradient pulse duration (δ) and 47.1 ms diffusion time (Δ), which was the interval between onsets of diffusion gradient pulses. Each DW image of a maximum of four phantoms was taken at about each 1 °C interval to cover the physiological body temperature within the range from 28 to 39 °C.

Accurate measurement of ADC values

We placed the regions of interest (ROIs; Fig. 1(F)) 7.27 mm square at the position of the thermometer on each phantom DW image. The averaged signal intensity in each ROI was obtained using Image-J software (National Institutes of Health, Bethesda, MD). The logarithms of these signal intensities were plotted as a function of the 11 b-values of 0, 300, 600, 900, 1200, 1500, 1800, 2100, 2400, 2700, and 3000 s/mm^2. The slope of the regression line, which is defined as the ADC value, and its R^2 value were obtained by the least-squares method. The ten sets of ADC values and their R^2 values were obtained for each set of data from 11 DW images using 11 b-values to 2 DW images using 2 b-values in order of decreasing b-values. When R^2 values exceeded 0.99 according to a decrease in b-values, the ADC values from its set of b-values was defined to be accurate; that is, we used the b-value within the range that the signal intensities

remained above the noise, and the slope of the logarithms of the signal intensities versus b-values became linear. We used these accurate ADC values to create the following empirical formula.

Empirical formula for calculating phantom ADC values

ADC values of phantoms were plotted as a function of temperature from 28–39 °C at 1° intervals for each sucrose concentration of 0, 0.2, 0.4, 0.6, 0.8, 1.0, and 1.2 M. The linear equations were made for each sucrose concentration based on a first-order approximation of the relationship between the ADC values and phantom temperature. First-order coefficients and intercepts of the seven linear equations were also plotted as a function of sucrose concentrations. Two formulas were then created, with one based on the fourth-order approximation of the relationship between first-order coefficients and sucrose concentrations, and another between intercepts and sucrose concentrations. Using these two formulas, an empirical formula was created for calculating ADC values of phantoms that were made of arbitrary sucrose concentrations at arbitrary phantom temperatures.

Accuracy validation of the empirical formula

To validate the accuracy of the empirical formula, we created new phantoms using sucrose concentrations of 0.2, 0.4, 0.6, 0.8, 1.0, and 1.2 M. We made three phantoms using all sucrose concentrations three times independently, and obtained mean ADC values at each concentration. The ADC values of these verification phantoms were measured at phantom temperatures ranging from 28–39 °C at 1° intervals. We compared the experimental mean ADC values of these verification phantoms and the ADC values calculated with the empirical formula by substituting sucrose concentrations and phantom temperatures at measurement, and then validated the relationship between ADC values calculated with the empirical formula and the range of standard deviations of the experimental ADC values of the verification phantoms.

Results

Calculation accuracy of ADC values

For each concentration and temperature of the sucrose phantom, ADC values were calculated. The ten sets of ADC values and their R^2 values were obtained by the least-squares method for each set of data from 11 DW images using 11 b-values to 2 DW images using 2 b-values in order of decreasing b-values. Figure 2 indicates the

calculation procedure of the ADC value of a 0.2 M phantom at a temperature of 37.09°C as an example. Among ten sets of ADC values and their R^2 values, when the maximum b-value decreased to 1500 s/mm^2 (Fig. 2(E)), the R^2 value obtained for the set of data from 6 DW images using 6 b-values exceeded 0.99 to become 0.9935. According to the slope calculation using this set, the ADC value of the 0.2 M phantom became 3.72×10^{-3}, which was decided to be accurate. Finally, ADC values were decided for all concentrations and temperatures as shown in Fig. 3(A).

Change of ADC values of sucrose phantoms by temperature

ADC values of 0, 0.2, 0.4, 0.6, 0.8, 1.0 and 1.2 M phantoms were plotted in Fig. 3(A) as a function of temperature. The ADC values of phantoms of each sucrose concentration rose as phantom temperature increased. The increasing rate of the ADC value per 1°C increased as the sucrose concentration decreased.

Development of an empirical formula to calculate ADC values

We made seven linear equations based on a first-order approximation of the relationship between the ADC values and phantom temperature (t) for each sucrose concentration (s) as shown in Fig. 3(A). The values of these R^2 were within the range of 0.9379–0.9801. First-order coefficients (A) and intercepts (B) of the seven linear equations were plotted as a function of sucrose concentrations (s) as shown in Fig. 3(B) and 3(C), respectively. We created each formula based on a fourth-order approximation of the relationship between first-order coefficients, or intercepts and sucrose concentrations. R^2 values were 0.9638 and 0.9862, respectively. Using these relational formulas, we created an empirical formula for calculating the ADC values of phantoms made of arbitrary sucrose concentration (s) at arbitrary phantom temperature (t), as follows:

ADC value ($\times 10^{-3}$ mm^2/sec) = At + B

$A = a_1s^4 - a_2s^3 + a_3s^2 - a_4s + a_5$

$a_1 = 8.96519842127907 \times 10^{-7}$,

$a_2 = 2.94479295800953 \times 10^{-5}$,

$a_3 = 6.94789261608819 \times 10^{-5}$,

$a_4 = 6.5038339758676 \times 10^{-5}$,

$a_5 = 6.22597789270809 \times 10^{-5}$

$B = -b_1s^4 + b_2s^3 - b_3s^2 + b_4s + b_5$

$b_1 = 5.75284527700504 \times 10^{-4}$,

$b_2 = 2.48741270074326 \times 10^{-3}$,

$b_3 = 3.12590711150129 \times 10^{-3}$,

$b_4 = 1.19937338765919 \times 10^{-4}$,

$b_5 = 5.94518521028771 \times 10^{-4}$

Accuracy validation of empirical formula

Figure 4(A) indicates the calculated ADC values using the empirical formula shown as the three-dimensional graph with the relationship among ADC values, sucrose concentration, and phantom temperature. The ADC values decrease according to an increase in sucrose concentration and decrease in phantom temperature. Figure 4(B) indicates the relationship between the ADC values, which have been used to make the empirical formula, and the ADC values calculated using the empirical formula. The formula seems to mimic well all ADC values that have been used to create it initially. Figure 4(C) indicates the relationship between the ADC values measured using verification phantoms and the ADC values calculated using the empirical formula. 66.67% of calculated ADC values were less than one standard deviation (SD) away from the mean of measured ADC values of verification phantoms; 97.22% of calculated ADC values were less than two SDs away from the mean, and 100% of calculated ADC values were less than 3 SDs away from the mean.

Discussion

To the best of our knowledge, this is the first study of the ADC phantoms for DWIs with 3T MR imaging. We created the ADC phantoms for 3T MRI using sucrose, and made an empirical formula for calculating ADC values between 0.33–3.02 × 10^{-3} at arbitrary sucrose concentrations between 0–1.2 M and arbitrary phantom temperature between 28–39 °C including a physiological temperature of 37 °C to mimic normal and tumor tissue of the human body.

Sucrose, a large molecule with the formula $C_{12}H_{22}O_{11}$, is a safe and inexpensive material, and it is easy to adjust the concentration of its solution. The diffusion coefficient of the material (D) was related to the temperature (t), the viscosity of the medium (η), and the radius of the diffusion molecule (r) with the Stokes-Einstein equation (11): $D = kt / 6\pi\eta r$, where k is the Boltzmann constant (1.3805×10^{-23} J K^{-1}). Therefore, we selected the sucrose that has a large molecular size, 0.9 nm in diameter, as the material of phantoms to decrease the ADC values (12).

According to Stokes-Einstein equation, ADC values are affected by the temperature of

the objects in question. As the ADC values used in clinical MR diagnosis are measured for the human body at 37 °C, ADC phantoms that mimic human body tissue should be comparable. Sasaki *et al.* (13) measured the ADC values of bio-phantoms using human Burkitt's lymphoma cells at 37 °C, otherwise most *in vitro* studies performed the ADC measurement at a lower temperature (14-16). Tamura, *et al.* (9) reported an ADC phantom using 10–50 wt% sucrose for 1.5T MRI, which cover the range of ADC values between 0.2–1.8 × 10^{-3} mm^2/s for temperatures between 6–20 °C. In our pre-examination, we measured the ADC values at temperatures from 6–39 °C. The R^2 values of the first-order approximation of the relationship between the ADC values and phantom temperature were low for phantoms of high sucrose concentration at temperatures < 27 °C. Therefore, we used a range of temperature between 28–39 °C to create an empirical formula.

This empirical formula covered ADC values from 0.672.47 × 10^{-3} mm^2/sec at a physiological temperature of 37 °C. Our ADC phantoms nearly covered the ADC values of normal and tumor tissues of the human body that are measured clinically by 3T MRI as summarized in Table 1 (1,3,5-8,17-19). The table indicates sucrose concentration of ADC phantoms at 37°C, which mimic each tissue of the human body by using our empirical formula.

One limitation of this study is that our sucrose phantom produces an ADC value due to change in free diffusion alone. The actual *in vivo* diffusion in the human body is affected by not only the change of free diffusion but also various factors including perfusion and the change of restricted diffusion due to cellular membrane structures, cell density, etc (20-26). This new ADC phantom and the empirical formula for 3T MRI has potential to be used in many applications.

Acknowledgements

We would like to thank the staff members of the Department of Radiology and Central Division of Radiology of Okayama University Hospital for their support of this study. This study was partially supported by a Grant-in-Aid for Scientific Research [C (22591335)] from the Ministry of Health, Labour and Welfare of Japan.

References

[1] Srinivasan A, Dvorak R, Rohrer S, Mukherji SK. Initial experience of 3-tesla apparent diffusion coefficient values in characterizing squamous cell carcinomas of the head and neck. Acta Radiol 49: 1079-84, 2008.

[2] Jung SH, Heo SH, Kim JW, Jeong YY, Shin SS, Soung MG, et al. Predicting response to neoadjuvant chemoradiation therapy in locally advanced rectal cancer: diffusion-weighted 3 Tesla MR imaging. J Magn Reson Imaging 35: 110-6, 2012.

[3] Kim HS, Kim CK, Park BK, Huh SJ, Kim B. Evaluation of therapeutic response to concurrent chemoradiotherapy in patients with cervical cancer using diffusion-weighted MR imaging. J Magn Reson Imaging 37: 187-93, 2013.

[4] Jensen LR, Garzon B, Heldahl MG, Bathen TF, Lundgren S, Gribbestad IS. Diffusion-weighted and dynamic contrast-enhanced MRI in evaluation of early treatment effects during neoadjuvant chemotherapy in breast cancer patients. J Magn Reson Imaging 34: 1099-109, 2011.

[5] Abdel Razek AA, Elkhamary S, Al-Mesfer S, Alkatan HM. Correlation of apparent diffusion coefficient at 3T with prognostic parameters of retinoblastoma. AJNR Am J Neuroradiol 33: 944-8, 2012.

[6] Doskaliyev A, Yamasaki F, Ohtaki M, Kajiwara Y, Takeshima Y, Watanabe Y, et al. Lymphomas and glioblastomas: Differences in the apparent diffusion coefficient evaluated with high b-value diffusion-weighted magnetic resonance imaging at 3T. Eur J Radiol 81: 339-44, 2012.

[7] Mottola JC, Sahni VA, Erturk SM, Swanson R, Banks PA, Mortele KJ. Diffusion-weighted MRI of focal cystic pancreatic lesions at 3.0-Tesla: preliminary results. Abdom Imaging 37: 110-7, 2012.

[8] Uehara T, Takahama J, Marugami N, Takahashi A, Takewa M, Itoh T, et al. Visualization of ovarian tumors using 3T MR imaging: diagnostic effectiveness and difficulties. Magn Reson Med Sci 11: 171-8, 2012.

[9] Tamura T, Usui S, Akiyama M. [Investigation of a phantom for diffusion weighted imaging that controlled the apparent diffusion coefficient using gelatin and sucrose]. Nihon Hoshasen Gijutsu Gakkai Zasshi 65: 1485-93, 2009.

[10] Matsuya R, Kuroda M, Matsumoto Y, Kato H, Matsuzaki H, Asaumi J, et al. A new phantom using polyethylene glycol as an apparent diffusion coefficient standard for MR imaging. Int J Oncol 35: 893-900, 2009.

[11] Einstein A. Investigations on the Theory of the Brownian movement. Dover Publications, Inc., New York, NY: p81, 1956.

[12] Ramm LE, Whitlow MB, Mayer MM. Transmembrane channel formation by complement: functional analysis of the number of C5b6, C7, C8, and C9 molecules required for a single channel. Proc Natl Acad Sci U S A 79: 4751-5, 1982.

[13] Sasaki T, Kuroda M, Katashima K, Ashida M, Matsuzaki H, Asaumi J, et al. In vitro assessment of factors affecting the apparent diffusion coefficient of Ramos cells using bio-phantoms. Acta Med Okayama 66: 263-70, 2012.

[14] Anderson AW, Xie J, Pizzonia J, Bronen RA, Spencer DD, Gore JC. Effects of cell volume fraction changes on apparent diffusion in human cells. Magn Reson Imaging 18: 689-95, 2000.

[15] Roth Y, Ocherashvilli A, Daniels D, Ruiz-Cabello J, Maier SE, Orenstein A, et al. Quantification of water compartmentation in cell suspensions by diffusion-weighted and T(2)-weighted MRI. Magn Reson Imaging 26: 88-102, 2008.

[16] Pilatus U, Shim H, Artemov D, Davis D, van Zijl PC, Glickson JD. Intracellular volume and apparent diffusion constants of perfused cancer cell cultures, as measured by NMR. Magn Reson Med 37: 825-32, 1997.

[17] Kitajima K, Takahashi S, Ueno Y, Yoshikawa T, Ohno Y, Obara M, et al. Clinical utility of apparent diffusion coefficient values obtained using high b-value when diagnosing prostate cancer using 3 tesla MRI: comparison between ultra-high b-value (2000 s/mm(2)) and standard high b-value (1000 s/mm(2)). J Magn Reson Imaging 36: 198-205, 2012.

[18] Cihangiroglu M, Ulug AM, Firat Z, Bayram A, Kovanlikaya A, Kovanlikaya I. High b-value diffusion-weighted MR imaging of normal brain at 3T. Eur J Radiol 69: 454-8, 2009.

[19] Ilica AT, Artas H, Ayan A, Gunal A, Emer O, Kilbas Z, et al. Initial experience of 3 tesla apparent diffusion coefficient values in differentiating benign and malignant thyroid nodules. J Magn Reson Imaging 37: 1077-82, 2013.

[20] Lyng H, Haraldseth O, Rofstad EK. Measurement of cell density and necrotic fraction in human melanoma xenografts by diffusion weighted magnetic resonance imaging. Magn Reson Med 43: 828-36, 2000.

[21] Kim H, Morgan DE, Buchsbaum DJ, Zeng H, Grizzle WE, Warram JM, et al. Early therapy evaluation of combined anti-death receptor 5 antibody and gemcitabine in

orthotopic pancreatic tumor xenografts by diffusion-weighted magnetic resonance imaging. Cancer Res 68: 8369-76, 2008.

[22] Kamel IR, Bluemke DA, Ramsey D, Abusedera M, Torbenson M, Eng J, et al. Role of diffusion-weighted imaging in estimating tumor necrosis after chemoembolization of hepatocellular carcinoma. AJR Am J Roentgenol 181: 708-10, 2003.

[23] Lang P, Wendland MF, Saeed M, Gindele A, Rosenau W, Mathur A, et al. Osteogenic sarcoma: noninvasive in vivo assessment of tumor necrosis with diffusion-weighted MR imaging. Radiology 206: 227-35, 1998.

[24] Gibbs P, Liney GP, Pickles MD, Zelhof B, Rodrigues G, Turnbull LW. Correlation of ADC and T2 measurements with cell density in prostate cancer at 3.0 Tesla. Invest Radiol 44: 572-6, 2009.

[25] Guo AC, Cummings TJ, Dash RC, Provenzale JM. Lymphomas and high-grade astrocytomas: comparison of water diffusibility and histologic characteristics. Radiology 224: 177-83, 2002.

[26] Thoeny HC, De Keyzer F, Chen F, Ni Y, Landuyt W, Verbeken EK, et al. Diffusion-weighted MR imaging in monitoring the effect of a vascular targeting agent on rhabdomyosarcoma in rats. Radiology 234: 756-64, 2005.

Figure legends

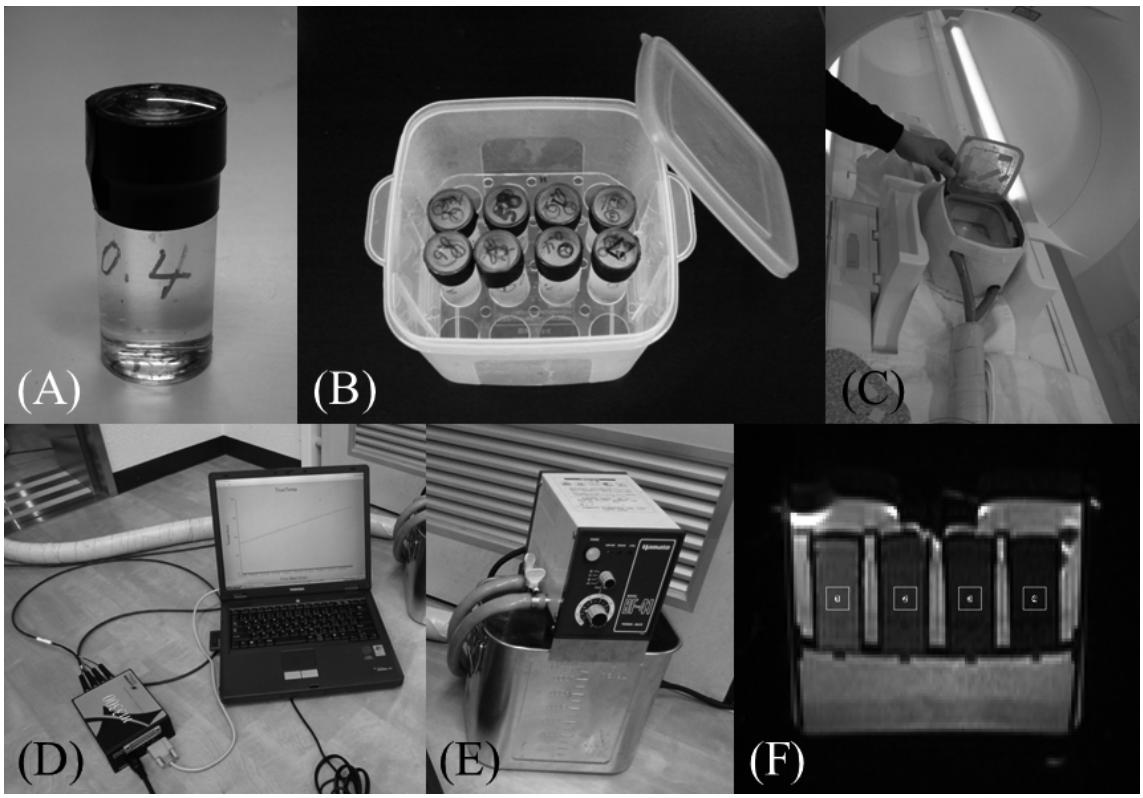

Figure 1. The phantom and methods for the experiments.

(A) The sucrose phantom in its case.

(B) The phantom case container. Up to 16 sucrose phantoms could be placed into this container filled with 0.9 M sucrose solution including 0.03 w/w% NaN_3.

(C) The heating box made of Styrofoam, which encloses the phantom case container. The container could be heated in the MR gantry via a tube that was connected to a circulating temperature-regulated water bath.

(D) The circulating temperature-regulated water bath.

(E) The optical fiber thermometer for temperature monitoring, which was put in a phantom.

(F) The ROIs 7.27 mm square at the position of the thermometer on each DW image.

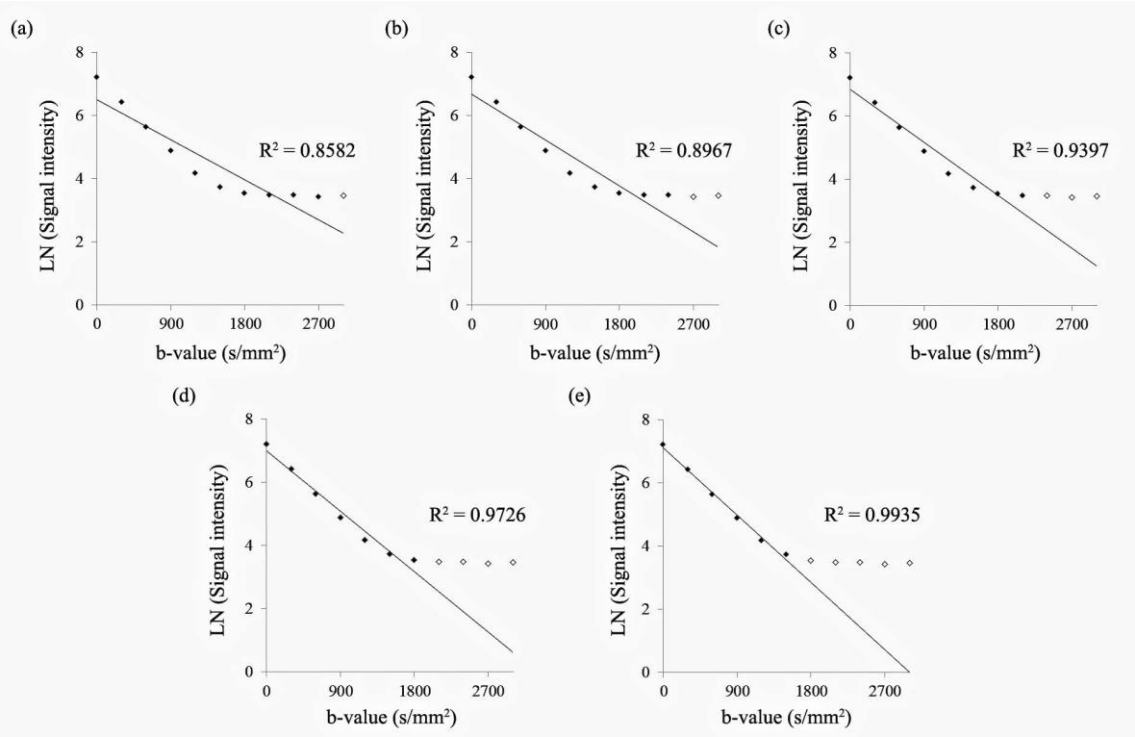

Figure 2. Calculation of ADC values of a 0.2 M phantom at 37.09 °C.

The vertical axis indicates the logarithm of the signal intensity of the ROI in the DW image of the phantom. The horizontal axis indicates b-values. ♦: The data that were used for the least-squares method to obtain the regression line and the R^2 value. ◊: The data that were not used for the least-squares method to obtain the regression line and the R^2 value.

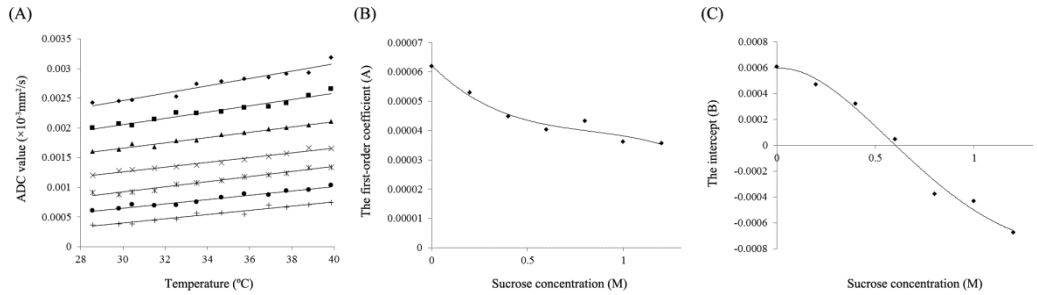

Figure 3. The ADC values of phantoms, and the development of an empirical formula to calculate the ADC values.

(A) The change of ADC values by temperature.

The vertical axis indicates the ADC values. The horizontal axis indicates phantom temperature.

♦: 0, ■: 0.2, ▲: 0.4, ×: 0.6, ✻: 0.8, ●: 1.0 and ＋: 1.2 M sucrose phantom. Each straight line indicates a first-order approximation of the relationship between ADC values and the phantom temperature for each sucrose concentration. The first-order coefficients and the intercepts of these linear equations are plotted on (B) and (C), respectively. Each R^2 value for the first-order approximation was within the range of 0.9379–0.9801.

(B) The relationships between the sucrose concentrations and the first-order coefficients of linear equations from the first-order approximation. Black diamonds indicate first-order coefficients. The curved line indicates the fourth-order approximation, with $R^2 = 0.9638$.

(C) The relationships between sucrose concentrations and the intercepts of the linear equations from the first-order approximation. Black diamonds indicate intercepts. The curved line indicated the fourth-order approximation, with $R^2 = 0.9862$.

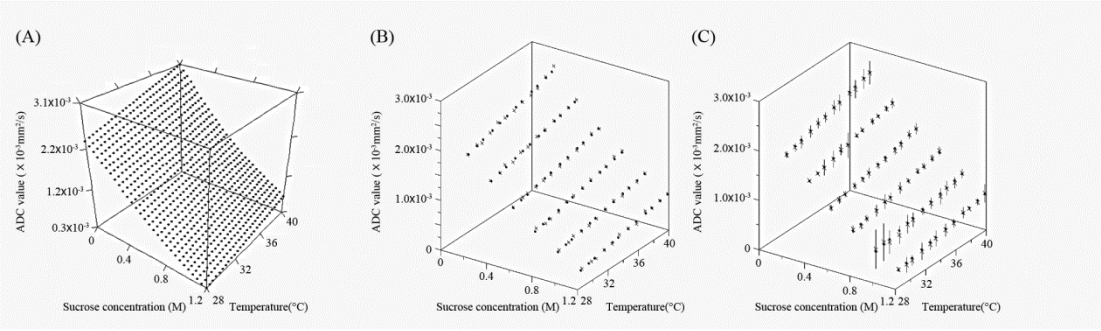

Figure 4. Calculated ADC values and accuracy validation using the empirical formula.

The vertical axis indicates the ADC values. The horizontal axes indicate sucrose concentration and phantom temperature, respectively. Black cubes in each figure indicate the ADC values that were calculated from the empirical formula.

(A) The ADC values which were calculated from the empirical formula.

(B) The relationship between predetermined and calculated ADC values using the empirical formula. The crosses (×) indicate the ADC values used to make the empirical formula.

(C) The relationship between the ADC values measured using verification phantoms and the ADC values calculated using the empirical formula. The crosses (×) and vertical lines indicate the mean and three standard deviations of the ADC values measured using verification phantoms.

Table 1. Sucrose concentration mimicking ADC values of human body

Regions	Mean ADC values ($\times 10^{-3} mm^2/sec$)	Sucrose concentration (M)
Lesions		
Brain		
Lymphoma[6]	0.62[*2]	1.2($\approx 0.6 \times 10^{-3} mm^2/sec$)
Head and neck		
Squamous cell carcinoma[1]	1.1	0.86
Thyroid gland		
Malignant tumor[19]	0.81[*3]	1.07
Benign tumor[19]	1.55[*3]	0.6
Pancreas		
neoplastic cystic lesion[7]	2.6[*2]	
mucinous cystic lesion[7]	2.6[*2]	
Uterin cervix		
Malignant tumor[3]	0.88[*2]	1.02
Ovary		
Malignant tumor[8]	1.04[*1]	0.91
Benign tumor[8]	1.15[*1]	0.84
Prostate		
Peripheral zone tissue		
Malignant tumor[17]	0.85[*4]	1.04
Benign tumor[17]	1.17[*4]	0.82
Transition zone tissue		
Malignant tumor[17]	0.84[*4]	1.05
Benign tumor[17]	1.08[*4]	0.88
Normal tissues		
Brain		
White matter[18]	0.76[*2]	1.11
Gray matter[18]	0.78[*2]	1.1
Muscle		

Gluteus[3]	1.24[*1]	0.78
Prostate		
Central gland[17]	1.19[*4]	0.81
Peripheral gland[17]	1.54[*4]	0.61
Tyroid tissue[19]	1.32[*3]	0.73

b-values (sec/mm^2): [*1] 0-800, [*2] 0-1000, [*3] 0-1500, [*4] 0-2000

The superscript at region is the number of reference.